A Particle-Mesh Method for the Shallow Water Equations Near Geostrophic Balance

Jason Frank[1] * and Sebastian Reich[2] †
* *CWI,P.O. Box 94079, 1090 GB Amsterdam*
† *Imperial College, Dept. of Mathematics, 180 Queen's Gate, London, SW7 2BZ*
E-mail: jason@cwi.nl, s.reich@ic.ac.uk

Version: 24 Jan. 2002

In this paper we outline a new particle-mesh method for rapidly rotating shallow-water flows, based on a set of regularized equations of motion. The time-stepping uses an operator splitting of the equations into an Eulerian gravity wave part and a Lagrangian advection part. An essential ingredient is the advection of absolute vorticity by means of translated radial basis functions. We show that this implies exact conservation of enstrophy. The method is tested on two model problems, based on qualitative features of the solutions obtained (i.e. dispersion or smoothness of PV contours) as well as increase in mean divergence level.

Key Words: geophysical fluid dynamics, potential vorticity conserving methods, particle-mesh methods

1. INTRODUCTION

The dynamics of the atmosphere is characterized by the existence of motion on two scales: the relatively slow advection of vortical structures and the relatively fast motion of gravity waves. The interaction between these types of motion is the subject of much current research in geophysical fluid dynamics. We expect that their proper numerical treatment is crucial both to an understanding of the motions in their own right and for obtaining meaningful results from long time simulations, for example, in climate studies.

The complete dynamics of the atmosphere are given by the three-dimensional primitive equation model. However, a simplified model which still retains much of the important dynamics of geophysical fluids is the rotating shallow water equations (SWEs):

$$\frac{d}{dt}\mathbf{u} = -f_0\mathbf{u}^{\perp} - c_0 H_0 \boldsymbol{\nabla}_{\boldsymbol{x}} h, \tag{1}$$

$$\frac{d}{dt}h = -(1+h)\boldsymbol{\nabla}_{\boldsymbol{x}} \cdot \mathbf{u}, \tag{2}$$

where $\mathbf{u} = (u,v)^T$ is the horizontal velocity field, $\mathbf{u}^{\perp} = (-v,u)^T$; h is the normalized layer depth variation; H_0 is the mean layer depth, i.e., the total layer depth is

[1]Partial support of GMD is gratefully acknowledged.
[2]Partial financial support by EPSRC Grant GR/R09565/01 and by European Commision funding for the Research Training Network "Mechanics and Symmetry in Europe is gratefully acknowledged.

$H = H_0(1+h)$; $f_0/2 > 0$ is the angular velocity of the reference plane; $c_0 > 0$ is an appropriate constant [14]; and $\frac{d}{dt} = \frac{\partial}{\partial t} + \mathbf{u}\cdot\boldsymbol{\nabla}_{\boldsymbol{x}}$ is the material time derivative.

In this paper, we consider the SWEs over a periodic domain $(x,y) \in [0,2\pi] \times [0,2\pi]$ with mean layer-depth $H_0 = 1$ and Rossby deformation radius $L_R = \sqrt{c_0 H_0}/f_0 = 1$. This scaling essentially leaves the Froude number

$$\varepsilon = \frac{1}{\sqrt{c_0 H_0}}$$

a free parameter. We introduce the scaled layer depth variation $\eta = \sqrt{c_0 H_0}h$ and rewrite the SWEs (1)–(2) as

$$\varepsilon \frac{d}{dt}\mathbf{u} = -L_R^{-1}\mathbf{u}^{\perp} - \boldsymbol{\nabla}_{\boldsymbol{x}}\eta, \tag{3}$$

$$\varepsilon \frac{d}{dt}\eta = -(1+\varepsilon\eta)\boldsymbol{\nabla}_{\boldsymbol{x}}\cdot\mathbf{u}. \tag{4}$$

We are mainly interested in problems with ε less than one.

A dynamical quantity of significant importance in geophysical fluid dynamics is the potential vorticity (PV)

$$Q = \frac{1+\varepsilon L_R \zeta}{1+\varepsilon\eta}, \qquad \zeta = v_x - u_y = \boldsymbol{\nabla}_{\boldsymbol{x}} \times \mathbf{u},$$

which is constant along particle trajectories; i.e. $dQ/dt = 0$. In the sequel, we will use the normalized potential vorticity

$$q = \frac{Q-1}{\varepsilon} = \frac{L_R\zeta - \eta}{1+\varepsilon\eta}.$$

The importance attached to PV in atmospheric dynamics is evidenced by its central role in quasigeostrophic theory. In extratropical regions, the terms on the right side of (3) are nearly in balance. This motivates the definition of the geostrophic wind

$$\mathbf{u}^{\mathrm{g}} = L_R \boldsymbol{\nabla}_{\boldsymbol{x}}^{\perp}\eta. \tag{5}$$

Note that if we assume (5), then the layer depth variation η can be recovered from the PV distribution via

$$(1+\varepsilon\eta)q = L_R^2 \boldsymbol{\nabla}_{\boldsymbol{x}}^2 \eta - \eta. \tag{6}$$

If we also make the assumption that $1 + \varepsilon\eta \approx 1$, then (6) gives rise to the linear relation

$$\eta = -\left(1 - L_R^2 \boldsymbol{\nabla}_{\boldsymbol{x}}^2\right)^{-1} q, \tag{7}$$

which is called PV inversion. Furthermore, the PV field itself is advected under the geostrophic flow field:

$$\frac{\partial q}{\partial t} + \mathbf{u}^{\mathrm{g}} \cdot \boldsymbol{\nabla}_{\boldsymbol{x}} q = 0. \tag{8}$$

The combined system (5), (7) and (8) is referred to as the quasigeostrophic approximation [14].

From a computational viewpoint it is important to notice that PV serves as a main organizing quantity of geostrophic flows. Accurate advection of the PV field is therefore of primary importance. This has been demonstrated using the contour-advective semi-Lagrangian (CASL) algorithm [3]. The CASL algorithm advects the PV field along Lagrangian particles that delineate contour lines of constant PV. The time evolution of the divergence $\delta = \nabla_{\boldsymbol{x}} \cdot \mathbf{u}$ and the layer depth variation η are computed over an Eulerian grid using a hierarchy of nonlinear balance conditions [12, 2]. The contour-advection schemes have been shown to result in a higher PV-field resolution compared to classical pseudospectral and semi-Lagrangian methods [12].

In addition to PV conservation, another computational challenge is the coexistence of fast (small amplitude) non-balanced motion and slow motion in geostrophic balance [14, 1, 9]. The geostrophic wind (5) is divergence-free. In contrast, the generation of (fast) unbalanced gravity waves is characterized by the divergence δ. In this paper, we are interested in smooth, nearly balanced motion, i.e., we assume that

$$\frac{d}{dt}\mathbf{u} = \mathcal{O}(\varepsilon^0) \qquad \text{and} \qquad \frac{d}{dt}\eta = \mathcal{O}(\varepsilon^0)$$

in (3)–(4). This implies, in particular, that $\delta = \mathcal{O}(\varepsilon)$.

One might wonder why PV and not relative vorticity ζ is used as a basic variable in geostrophic theory. Indeed, we obtain

$$\zeta_t + \mathbf{u}^{\mathrm{g}} \cdot \nabla_{\boldsymbol{x}} \zeta = -\varepsilon^{-1} L_R^{-1} \delta$$

to leading orders in ε. To close the equation, one needs an order $\mathcal{O}(\varepsilon)$ approximation to the divergence δ, which is provided by (see §5)

$$\delta = -\varepsilon L_R \left(1 - L_R^2 \nabla_{\boldsymbol{x}}^2\right)^{-1} \left[\mathbf{u}^{\mathrm{g}} \cdot \nabla_{\boldsymbol{x}} \zeta\right].$$

Hence we obtain the vorticity equation

$$\left(1 - L_R^2 \nabla_{\boldsymbol{x}}^2\right) \zeta_t - L_R^2 \mathbf{u}^{\mathrm{g}} \cdot \nabla_{\boldsymbol{x}} \nabla_{\boldsymbol{x}}^2 \zeta = 0 \tag{9}$$

with the geostrophic wind now determined by

$$\mathbf{u}^{\mathrm{g}} = \nabla_{\boldsymbol{x}}^{\perp} \nabla_{\boldsymbol{x}}^{-2} \zeta.$$

The vorticity equation (9) is clearly more complex than the PV equation (8). However no PV inversion (7) is required. This fact will be explored in the design of the new method. It is one of the central ideas of this paper that vorticity can easily be advected along the full equations (3)–(4).

In this paper we outline a new numerical method for the SWEs that respects the above considerations of PV conservation and balance; the generalized enstrophies are conserved. Additionally, the new method utilizes recent ideas on fine scale spatial averaging. Finally, the new method is conservative (i.e. reversible) and efficient to implement (i.e. explicit and one-step). To accomplish these goals, we apply simplifying assumptions to the SWEs, in two steps:

(i) Geometric Remodelling, (ii) Geometric Integration

In Step (i) (Section 2), we derive regularized SWEs, under a nearly geostrophic assumption $\varepsilon \ll 1$, in which the fine scale velocity fluctuations are filtered out according to recent ideas from Lagrangian mean flow theory and averaged Euler equations (see, e.g., [1] and [7]), while still preserving the "geometric" constraints of PV, mass, and energy conservation. The idea of filtered equations is also utilized, for example, in large eddy simulations (LES).

In Step (ii) (Section 3), we rewrite the modified SWEs in vorticity-divergence variables and introduce additional geostrophic assumptions to cast the resulting model in a form suitable for reversible, explicit, one-step integration via an operator splitting—into a semi-linear (fast) wave equation and an advection step—that takes the importance of geostrophic balance into account and that can be implemented using an appropriate modification of a particle-mesh (PM) [6] or particle-in-cell (PIC) method [5]. Contrary to PV contour-advection, we advect the absolute vorticity $\omega = 1 + \varepsilon L_R \zeta$ using radial basis functions and Lagrangian particle dynamics. As opposed to some other Lagrangian approaches, we did not need to regularly redistribute the particles in our numerical experiments. The semi-linear wave equation is solved over a fixed Eulerian grid.

The main feature of the new method, as demonstrated by a series of numerical experiments in Section 5, is to capture balanced motion as well as to predict the long time dynamics of the PV field. We show that the generalized enstrophies, which we define as

$$\mathcal{Q}_f = \int \{\omega\, f(q)\}\, dx \wedge dy \tag{10}$$

where $\omega = 1 + \varepsilon L_R \zeta$ is the absolute vorticity, are exactly conserved over the (x, y)-domain for any function $f(q)$.

2. GEOMETRIC REMODELLING: A REGULARIZED SWE FORMULATION

In this section we apply geostrophic assumptions to the SWEs and reformulate them to include advection field regularization based on Lagrangian mean theory [7]. The resulting model retains PV, energy and mass conservation, and the regularized velocity field satisfies the geostrophic condition (5) as $\varepsilon \to 0$. The regularized system differs from (3)–(4) by terms of order $\mathcal{O}(\varepsilon^2)$.

The SWEs (3)–(4) can be written as an infinite-dimensional Hamiltonian system of the form

$$\varepsilon \begin{pmatrix} \mathbf{u}_t \\ \eta_t \end{pmatrix} = \begin{pmatrix} -L_R^{-1} Q \mathbf{e}_z \times & -\boldsymbol{\nabla}_{\boldsymbol{x}} \\ -\boldsymbol{\nabla}_{\boldsymbol{x}} \cdot & 0 \end{pmatrix} \begin{pmatrix} \delta\mathcal{E}/\delta\mathbf{u} \\ \delta\mathcal{E}/\delta\eta \end{pmatrix} \tag{11}$$

with Hamiltonian

$$\mathcal{E} = \frac{1}{2} \int \left\{ (1 + \varepsilon\eta)\mathbf{u} \cdot \mathbf{u} + \eta^2 \right\} dx \wedge dy. \tag{12}$$

We first assume that the fluid flow is almost incompressible, i.e., we assume $1 + \varepsilon\eta \approx 1$ in (12). Next note that

$$\frac{1}{2}\eta^2 = \varepsilon^{-2} \left[(1 + \varepsilon\eta)(\ln(1 + \varepsilon\eta) - 1) + 1 \right] + \mathcal{O}(\varepsilon).$$

Furthermore, it is well-known that the velocity field $\mathbf{u}$ develops increasingly fine structures as time evolves. On the other hand, a truncation can only resolve spatial structures up to a certain length-scale $\alpha \sim \Delta x = \Delta y$. Following recent advances on averaged Euler fluid models [7], this suggests to smooth/average the velocity field over all length-scales smaller than α. Hence we replace the Hamiltonian (12) by the modified energy

$$\mathcal{E}_\alpha = \frac{1}{2} \int \left\{ (\mathcal{S}_\alpha^{p/2}\mathbf{u}) \cdot (\mathcal{S}_\alpha^{p/2}\mathbf{u}) + 2\varepsilon^{-2} \left[(1+\varepsilon\eta)(\ln(1+\varepsilon\eta) - 1) + 1 \right] \right\} dx \wedge dy, \quad (13)$$

where S_α^ν denotes the operator

$$\mathcal{S}_\alpha^\nu = \left(1 - \alpha^2 \boldsymbol{\nabla}_{\boldsymbol{x}}^2\right)^{-\nu}$$

and p is a positive integer. Averaged Euler models typically use $p = 1$. In our numerical experiments, however, we worked with $p = 1$, $p = 2$, and $p = 4$. Given some spatial discretization with spatial increment Δx, we set $\alpha = c\Delta x$, $c \geq 1$. Hence we have $\alpha \to 0$ as $\Delta x \to 0$ and the regularization can be thought of as part of the spatial truncation process.

Note that

$$\frac{\delta \mathcal{E}_\alpha}{\delta \eta} = \varepsilon^{-1} \ln(1+\varepsilon\eta) \quad \text{and} \quad \frac{\delta \mathcal{E}_\alpha}{\delta \mathbf{u}} = \mathcal{S}_\alpha^p \mathbf{u}.$$

This suggests defining the modified equations of motion by

$$\varepsilon \begin{pmatrix} \mathbf{u}_t \\ \eta_t \end{pmatrix} = \begin{pmatrix} -L_R^{-1} \omega \mathbf{e}_z \times & -(1+\varepsilon\eta)\boldsymbol{\nabla}_{\boldsymbol{x}} \\ -\boldsymbol{\nabla}_{\boldsymbol{x}} \cdot (1+\varepsilon\eta) & 0 \end{pmatrix} \begin{pmatrix} \delta\mathcal{E}_\alpha/\delta\mathbf{u} \\ \delta\mathcal{E}_\alpha/\delta\eta \end{pmatrix}, \quad (14)$$

which are equivalent to the modified SWEs

$$\varepsilon \mathbf{u}_t = -L_R^{-1} \omega (\mathcal{S}_\alpha^p \mathbf{u})^\perp - \boldsymbol{\nabla}_{\boldsymbol{x}} \eta, \quad (15)$$

$$\varepsilon \eta_t = -\boldsymbol{\nabla}_{\boldsymbol{x}} \cdot ((1+\varepsilon\eta)\mathcal{S}_\alpha^p \mathbf{u}), \quad (16)$$

where

$$\omega = 1 + \varepsilon L_R \zeta$$

is the absolute vorticity.

Let us introduce the modified material derivative

$$\frac{D}{Dt}(\cdot) = \frac{\partial}{\partial t}(\cdot) + \mathbf{v} \cdot \boldsymbol{\nabla}_{\boldsymbol{x}}(\cdot)$$

along the smoothed velocity field

$$\mathbf{v} = \mathcal{S}_\alpha^p \mathbf{u}.$$

Then one can extract from (15)–(16) the two continuity equations

$$\varepsilon \frac{D}{Dt}\eta = -(1+\varepsilon\eta)\boldsymbol{\nabla}_{\boldsymbol{x}} \cdot \mathbf{v}$$

and

$$\frac{D}{Dt}\omega = -\omega \boldsymbol{\nabla}_{\boldsymbol{x}} \cdot \mathbf{v}. \quad (17)$$

Hence the PV field $Q = \omega/(1+\varepsilon\eta)$ is still materially conserved, i.e., $DQ/Dt = 0$. The total energy (13) is also conserved. The equation for the divergence becomes

$$\varepsilon\delta_t = L_R^{-1}\omega\nabla_{\boldsymbol{x}} \times \mathbf{v} + L_R^{-1}\mathbf{v}\cdot\nabla_{\boldsymbol{x}}^{\perp}\omega - \nabla_{\boldsymbol{x}}^2\eta, \tag{18}$$

which, for $\alpha = 0$, reduces to its standard form except for the missing $-\varepsilon\nabla_{\boldsymbol{x}}^2(\mathbf{u}\cdot\mathbf{u})/2$ term. But note that

$$\mathbf{u}\cdot\mathbf{u} = L_R^2\nabla_{\boldsymbol{x}}\eta\cdot\nabla_{\boldsymbol{x}}\eta + \mathcal{O}(\varepsilon).$$

Hence, if we assume nearly geostrophic balance, i.e., $\delta = \mathcal{O}(\varepsilon)$, and replace η in the momentum equation (15) and in the continuity equation (16) by $\bar{\eta}$ with

$$\bar{\eta} = \eta + \frac{\varepsilon L_R^2}{2}\nabla_{\boldsymbol{x}}\eta\cdot\nabla_{\boldsymbol{x}}\eta,$$

then the resulting equations differ, for $\alpha = 0$, from (3)–(4) by terms of order $\mathcal{O}(\varepsilon^2)$. The statement is obvious for the momentum equation and for the continuity equation we obtain

$$\begin{aligned}
\varepsilon\bar{\eta}_t &= \varepsilon\eta_t + \varepsilon^2 L_R^2\nabla_{\boldsymbol{x}}\eta\cdot\nabla_{\boldsymbol{x}}\eta_t \\
&= -\nabla_{\boldsymbol{x}}\cdot((1+\varepsilon\eta)\mathbf{v}) - \varepsilon L_R^2\nabla_{\boldsymbol{x}}\eta\cdot\nabla_{\boldsymbol{x}}(\mathcal{S}_\alpha^p\delta) + \mathcal{O}(\varepsilon^2) \\
&= -\nabla_{\boldsymbol{x}}\cdot((1+\varepsilon\bar{\eta})\mathbf{v}) + \mathcal{O}(\varepsilon^2).
\end{aligned}$$

In this paper, we simply identify $\bar{\eta}$ with η.

One can again formally investigate the limit $\varepsilon \to 0$. For simplicity, we also set $p = 1$ in (13). We define the modified geostrophic wind

$$\mathbf{v}^{\mathrm{g}} = L_R\nabla_{\boldsymbol{x}}^{\perp}\eta$$

and obtain the PV relation ($\varepsilon = 0$):

$$q = L_R^2\mathcal{S}_\alpha^{-1}\nabla_{\boldsymbol{x}}\times\mathbf{v}^{\mathrm{g}} - \eta = -(1 - L_R^2\nabla_{\boldsymbol{x}}^2 + \alpha^2 L_R^2\nabla_{\boldsymbol{x}}^4)\eta.$$

PV is advected via

$$\frac{\partial q}{\partial t} + \mathbf{v}^{\mathrm{g}}\cdot\nabla_{\boldsymbol{x}} q = 0.$$

These equations are similar to the 2D averaged incompressible Euler equations [7, 8]. See [8] for a global existence and uniqueness result.

Various other averaged formulations of the shallow-water equations can be formulated. We mention, in particular, the Eulerian mean rotating shallow water (EMRSW) model of [7], which is of the form (15)–(16) with added terms in the momentum equation (15). The resulting equations of motion, although of slightly higher complexity, can also be implemented numerically using the techniques developed in §3. The advantage of the current model is that it lends itself to efficient numerical integration using a reversible, explicit one-step method as described in the next section.

3. GEOMETRIC INTEGRATION: THE BALANCED PARTICLE-MESH (BPM) METHOD

We now derive our new discretization method for the regularized SWEs (15)–(16) which we call the BALANCED PARTICLE-MESH (BPM) method. In Section 3.1, we first rewrite the SWEs in vorticity-divergence variables and make some additional assumptions of near-geostrophy, which simplify the coupling of the divergence and layer depth equations. Next, in Section 3.2 we discretize in time using a reversible, explicit, one-step splitting. Finally, in Section 3.3 we define the spatial discretization. Although we lose exact conservation of PV and energy in the following manipulations, we will see that the final method exactly conserves the generalized enstrophies (10).

3.1. The SWEs near geostrophic balance

Let $\bar{\mathbf{v}}$ denote the divergence-free part of the velocity field $\mathbf{v}$ and let us introduce the balanced layer-depth variation

$$\eta^{\mathrm{g}} = \eta^{\mathrm{g}}(\omega) = -L_R^{-1} \boldsymbol{\nabla}_{\boldsymbol{x}}^{-2} \boldsymbol{\nabla}_{\boldsymbol{x}} \cdot (\omega \bar{\mathbf{v}}^{\perp}), \tag{19}$$

which corresponds to $\boldsymbol{\nabla}_{\boldsymbol{x}} \cdot \mathbf{u}_t = \delta_t = 0$ in (18) under the assumption of $\delta^{\mathrm{s}} = \boldsymbol{\nabla}_{\boldsymbol{x}} \cdot \mathbf{v} = 0$.

We next reformulate the SWEs (15)–(16) in terms of $(\omega, \delta^{\mathrm{s}}, \eta)$ under the assumption $\delta^{\mathrm{s}} = \mathcal{O}(\varepsilon)$ and $\eta - \eta^{\mathrm{g}} = \mathcal{O}(\varepsilon)$ (nearly geostrophic balance). Since

$$\boldsymbol{\nabla}_{\boldsymbol{x}}^2 \eta^{\mathrm{g}} = -L_R^{-1} \boldsymbol{\nabla}_{\boldsymbol{x}} \cdot (\omega \mathbf{v}^{\perp}) + \mathcal{O}(\varepsilon^2),$$

we obtain

$$\varepsilon \delta_t^{\mathrm{s}} = -\mathcal{S}_\alpha^p \boldsymbol{\nabla}_{\boldsymbol{x}}^2 (\eta - \eta^{\mathrm{g}})$$

up to terms of order $\mathcal{O}(\varepsilon^2)$ which we ignore. In a similar manner, one can simplify the continuity equation (16) to

$$\varepsilon \eta_t = -\boldsymbol{\nabla}_{\boldsymbol{x}} \cdot ((1 + \varepsilon \eta^{\mathrm{g}}) \mathbf{v}).$$

Hence, the transformed system of equations consists of a semi-linear wave equation of the form

$$\varepsilon \eta_t = -(1 + \varepsilon A(\omega)) \delta^{\mathrm{s}} - \varepsilon g(\omega), \qquad \varepsilon \delta_t^{\mathrm{s}} = -\mathcal{S}_\alpha^p \boldsymbol{\nabla}_{\boldsymbol{x}}^2 (\eta - \eta^{\mathrm{g}}(\omega)), \tag{20}$$

together with the continuity equation (17) and the diagnostic relation (19).

The idea for numerical time-stepping is to represent absolute vorticity ω in terms of radial basis functions and to solve (17) using Lagrangian particles advected along the velocity field $\mathbf{v}$. The wave equation in $(\delta^{\mathrm{s}}, \eta)$ is truncated by a pseudospectral (PS) method over an Eulerian grid. The details will be described in the following subsections.

3.2. A fractional time-stepping method

The equations of motion in $(\omega, \delta^{\mathrm{s}}, \eta)$ are first split into an Eulerian part (20) and a Lagrangian part in which (17) is solved along the flow of

$$\frac{D}{Dt} \boldsymbol{x} = \mathbf{v}, \qquad \mathbf{v}_t = \mathbf{a}, \tag{21}$$

where $\mathbf{a}$ is the Eulerian particle acceleration

$$\mathbf{a} = -\varepsilon^{-1}\mathcal{S}_\alpha^p \left[L_R^{-1}\omega\mathbf{v}^\perp + \nabla_{\boldsymbol{x}}\eta\right].$$

To integrate (21) and (17), we introduce M Lagrangian (moving) particles with location $\{\boldsymbol{X}^k\}$ and velocity $\{\boldsymbol{V}^k\}$. Let us denote the Lagrangian particle positions at time level $t_{n+1/2}$ by $\boldsymbol{X}_{n+1/2}^k$ and the particle velocity at t_n by $\mathbf{V}_n^k$. In §3.3, we describe a radial basis function approach to obtain the vorticity $\omega_{n+1/2}$ at time level $t_{n+1/2}$ knowing the particle positions $\{\boldsymbol{X}_{n+1/2}^k\}$. Hence let us assume for now that $\omega_{n+1/2}$ is known.

Then the wave equation (20) is discretized in time via the time-symmetric discretization

$$\begin{aligned}
\delta_{n+1/2}^{\mathrm{s}} &= \delta_n^{\mathrm{s}} - \frac{\delta t}{2\varepsilon}\mathcal{S}_\alpha^p\nabla_{\boldsymbol{x}}^2(\eta_n - \eta_{n+1/2}^{\mathrm{g}}),\\
\eta_{n+1} &= \eta_n - \frac{\delta t}{\varepsilon}\left\{(1+\varepsilon A(\omega_{n+1/2}))\delta_{n+1/2}^{\mathrm{s}} + \varepsilon g(\omega_{n+1/2})\right\}, \qquad (22)\\
\delta_{n+1}^{\mathrm{s}} &= \delta_{n+1/2}^{\mathrm{s}} - \frac{\delta t}{2\varepsilon}\mathcal{S}_\alpha^p\nabla_{\boldsymbol{x}}^2(\eta_{n+1} - \eta_{n+1/2}^{\mathrm{g}}).
\end{aligned}$$

We would like to point out that a smaller time step $\delta t/K$ can be applied to the wave equation (20); effectively leading to a multiple-time-stepping method; i.e.

$$\begin{aligned}
\delta_{n+\frac{i+1/2}{K}}^{\mathrm{s}} &= \delta_{n+\frac{i}{K}}^{\mathrm{s}} - \frac{\delta t}{2\varepsilon K}\mathcal{S}_\alpha^p\nabla_{\boldsymbol{x}}^2(\eta_{n+\frac{i}{K}} - \eta_{n+1/2}^{\mathrm{g}}),\\
\eta_{n+\frac{i+1}{K}} &= \eta_{n+\frac{i}{K}} - \frac{\delta t}{\varepsilon K}\left\{(1+\varepsilon A(\omega_{n+1/2}))\delta_{n+\frac{i+1/2}{K}}^{\mathrm{s}} + \varepsilon g(\omega_{n+1/2})\right\},\\
\delta_{n+\frac{i+1}{K}}^{\mathrm{s}} &= \delta_{n+\frac{i+1/2}{K}}^{\mathrm{s}} - \frac{\delta t}{2\varepsilon K}\mathcal{S}_\alpha^p\nabla_{\boldsymbol{x}}^2(\eta_{n+\frac{i+1}{K}} - \eta_{n+1/2}^{\mathrm{g}})
\end{aligned}$$

for $i = 0, \dots, K-1$. This approach could be combined with the averaging ideas presented in [11].

Once $\delta_{n+1/2}^{\mathrm{s}}$, $\omega_{n+1/2}$, and $\eta_{n+1/2} = (\eta_{n+1} + \eta_n)/2$ are known, the smoothed Eulerian particle acceleration

$$\mathbf{a}_{n+1/2} = -\varepsilon^{-1}\mathcal{S}_\alpha^p\left[L_R^{-1}\omega_{n+1/2}\mathbf{v}_{n+1/2} + \nabla_{\boldsymbol{x}}\eta_{n+1/2}\right]$$

can be computed using the half-step velocity field

$$\mathbf{v}_{n+1/2} = \nabla_{\boldsymbol{x}}^\perp\nabla_{\boldsymbol{x}}^{-2}\mathcal{S}_\alpha^p\zeta_{n+1/2} + \nabla_{\boldsymbol{x}}\nabla_{\boldsymbol{x}}^{-2}\delta_{n+1/2}^{\mathrm{s}},$$

where $\zeta_{n+1/2} = \varepsilon^{-1}L_R^{-1}(\omega_{n+1/2} - 1)$.

The smoothed advection velocities $\mathbf{v}_n$ on the Eulerian grid are now updated via

$$\mathbf{v}_{n+1} = \mathbf{v}_n + \delta t\mathbf{a}_{n+1/2}$$

and then mapped onto the particles via a simple bilinear interpolation[3] to yield $\mathbf{V}_{n+1}^k$. Finally, the Lagrangian particle positions are updated via

$$\boldsymbol{X}_{n+3/2}^k = \boldsymbol{X}_{n+1/2}^k + \delta t\mathbf{V}_{n+1}^k.$$

[3] One could use a higher order interpolation, but since the advection velocity field is smoothed anyway, we found bilinear interpolation to be sufficient for the resolutions considered.

3.3. A spatial truncation and conservation of enstrophy

Since we work with double periodic boundary conditions, we can apply a standard pseudospectral discretization to truncate the equations (20). We will denote the number of Fourier modes in each spatial dimension by N, i.e., $\Delta x = \Delta y = 2\pi/N$.

The absolute vorticity ω satisfies a continuity equation of the form

$$\omega_t + \nabla_{\boldsymbol{x}} \cdot (\omega \mathbf{v}) = 0.$$

Hence, following the idea of smoothed particle hydrodynamics (SPH) [13], we assign each Lagrangian particle a vorticity density $\{\Omega_k\}$ and approximate ω at an Eulerian location $\boldsymbol{x}$ via the interpolation formula

$$\omega(\boldsymbol{x}, t_{n+1/2}) = \sum_k \Omega_k \psi\left(||\boldsymbol{x} - \boldsymbol{X}^k_{n+1/2}||^2\right) \tag{23}$$

where $\psi(z) \geq 0$ is an appropriate radial basis function and $\boldsymbol{X}^k_{n+1/2}$ is the kth particle position at $t_{n+1/2}$.

Let us explain this approach in more detail [15]. We assume, for simplicity, that

$$\omega(\boldsymbol{x}, t) = \sum_k \Omega_k \psi\left(||\boldsymbol{x} - \boldsymbol{X}^k(t)||^2\right) > 0.$$

Then each particle contributes the fraction

$$\rho_k(\boldsymbol{x}, t) = \frac{\Omega_k \psi\left(||\boldsymbol{x} - \boldsymbol{X}^k(t)||^2\right)}{\omega(\boldsymbol{x}, t)}$$

to the total vorticity. These fractions form a partition of unity, i.e.

$$\sum_k \rho_k(\boldsymbol{x}, t) = 1.$$

Hence they can be used to interpolate data from the particle locations to any $\boldsymbol{x}$. In particular, we define a continuous Eulerian velocity field

$$\mathbf{v}(\boldsymbol{x}, t) = \sum_k \rho_k(\boldsymbol{x}, t)\mathbf{V}^k(t)$$

and a vorticity flux density

$$\omega(\boldsymbol{x}, t)\mathbf{v}(\boldsymbol{x}, t) = \sum_k \Omega_k \psi\left(||\boldsymbol{x} - \boldsymbol{X}^k(t)||^2\right)\mathbf{V}^k(t).$$

Using $d\mathbf{X}^k/dt = \mathbf{V}^k$, it is now easily verified that

$$\frac{\partial}{\partial t}\omega(\boldsymbol{x}, t) + \nabla_{\boldsymbol{x}} \cdot (\omega(\boldsymbol{x}, t)\mathbf{v}(\boldsymbol{x}, t)) = 0.$$

The same argument can be used to derive conservation laws for the generalized enstrophy densities $\omega f(q)$. We associate with each particle a PV value of q_k. This give rise to generalized Eulerian PV fields

$$f(q)(\boldsymbol{x}, t) = \sum_k f(q_k)\, \rho_k(\boldsymbol{x}, t)$$

and the approximation

$$\omega(\boldsymbol{x},t)\, f(q)(\boldsymbol{x},t) = \sum_k (\Omega_k\, f(q_k))\, \psi\left(||\boldsymbol{x} - \boldsymbol{X}^k(t)||^2\right).$$

Hence we obtain

$$\frac{\partial}{\partial t}\left\{\omega(\boldsymbol{x},t)\, f(q)(\boldsymbol{x},t)\right\} = -\sum_k \boldsymbol{\nabla}_{\boldsymbol{x}} \cdot \left\{(\Omega_k\, f(q_k))\, \psi\left(||\boldsymbol{x} - \boldsymbol{X}^k(t)||^2\right) \mathbf{V}^k(t)\right\}$$

and exact conservation of the generalized enstrophies (10) under the given periodic boundary conditions.

Note that the BPM method does not exactly satisfy the relation

$$\omega = (1+\varepsilon\eta)Q, \qquad Q = 1 + \varepsilon q.$$

However, since the scaled layer-depth

$$\mathcal{H} = 1 + \varepsilon\eta$$

satisfies a continuity equation, one can apply the approximation

$$\mathcal{H}(\boldsymbol{x},t) = \sum_k m_k \psi\left(||\boldsymbol{x} - \boldsymbol{X}^k(t)||^2\right),$$

where $\{m_k\}$ are appropriate constants. Then, upon introducing the fractions

$$\rho_k(\boldsymbol{x},t) = \frac{m_k \psi\left(||\boldsymbol{x} - \boldsymbol{X}^k(t)||^2\right)}{\mathcal{H}(\boldsymbol{x},t)}$$

and the generalized Eulerian PV fields

$$f(Q)(\boldsymbol{x},t) = \sum_k f(Q_k)\, \rho_k(\boldsymbol{x},t),$$

where $Q_k = 1 + \varepsilon q_k$, we obtain the approximation

$$\mathcal{H}(\boldsymbol{x},t) f(Q)(\boldsymbol{x},t) = \sum_k (m_k\, f(Q_k))\, \psi\left(||\boldsymbol{x} - \boldsymbol{X}^k(t)||^2\right).$$

Obviously all of the generalized enstrophy densities again exactly satisfy conservation laws. Note that

$$\omega(\boldsymbol{x},t) = \mathcal{H}(\boldsymbol{x},t) Q(\boldsymbol{x},t) = \sum_k \Omega_k\, \psi\left(||\boldsymbol{x} - \boldsymbol{X}^k(t)||^2\right)$$

with $\Omega_k = m_k Q_k$. The time-stepping of the BPM method can still be applied with the only modification that (22) reduces to

$$\delta^s_{n+1} = \delta^s_n - \frac{\delta t}{\varepsilon} \mathcal{S}^p_\alpha \boldsymbol{\nabla}^2_{\boldsymbol{x}} (\varepsilon^{-1}\mathcal{H}(\boldsymbol{x}, t_{n+1/2}) - \eta^{\rm g}(\boldsymbol{x}, t_{n+1/2}))$$

and

$$\mathcal{H}(\boldsymbol{x}, t_{n+1/2}) = \sum_k m_k \psi\left(||\boldsymbol{x} - \boldsymbol{X}^k_{n+1/2}||^2\right).$$

as well as

$$\omega(\boldsymbol{x}, t_{n+1/2}) = \sum_k (m_k\, Q_k)\, \psi\left(||\boldsymbol{x} - \boldsymbol{X}^k_{n+1/2}||^2\right).$$

However, the idea of multiple-time-stepping and averaging seems more difficult to apply to this modified BPM scheme.

4. A PSEUDOSPECTRAL LEAPFROG-TRAPEZOIDAL DISCRETIZATION

For comparison purposes, we now describe a standard pseudospectral (PS) discretization of the modified SWEs (15)–(16). Introduce $\mathbf{w} = (\mathbf{u}^T, \eta)^T \in \mathbf{R}^3$ and write (15)–(16) in the abstract form

$$\mathbf{w}_t = \varepsilon^{-1}\boldsymbol{A}\mathbf{w} + \boldsymbol{f}(\mathbf{w}), \qquad \boldsymbol{A} = \begin{bmatrix} -L_R^{-1}\mathcal{S}_\alpha^p \mathbf{e}_z\times & -\boldsymbol{\nabla}_{\boldsymbol{x}} \\ -\mathcal{S}_\alpha^p \boldsymbol{\nabla}_{\boldsymbol{x}}\cdot & 0 \end{bmatrix}. \tag{24}$$

Spatial derivatives are computed in Fourier space using an FFT, and the product of any two functions is computed in physical space. The truncation is implemented such that the finite-dimensional system exactly conserves an approximation to the total energy.

The time-discretization is done using the leapfrog method for advection and the trapezoidal rule for the linear wave part (LF/TR):

$$\frac{\mathbf{w}^{n+1} - \mathbf{w}^{n-1}}{2\Delta t} = \varepsilon^{-1}\boldsymbol{A}\frac{\mathbf{w}^{n+1} + \mathbf{w}^{n-1}}{2} + f(\mathbf{w}^n). \tag{25}$$

This time-symmetric two-step method is started with one time step of an analogous implicit/explicit Euler step of size $\Delta t/2^K$, followed by K stationary applications of (25) each time restarting from the initial condition and doubling the step-size. We used $K = 10$ in the numerical experiments.

To obtain a smooth PV field it is usually necessary to include a hyperviscosity term in the momentum equation, replacing (15) with

$$\varepsilon\mathbf{u}_t = -L_R^{-1}\omega\mathbf{v}^\perp - \boldsymbol{\nabla}_{\boldsymbol{x}}\eta + \nu\left(\boldsymbol{\nabla}_{\boldsymbol{x}}^2\right)^3\mathbf{u}, \tag{26}$$

where the viscosity coefficient was taken to be:

$$\nu = \frac{100\,\varepsilon\,\bar{Q}}{(N/2)^6}, \qquad \max_{\boldsymbol{x}} |Q(\boldsymbol{x})| \le \bar{Q}.$$

The hyperviscosity term is discretized in time using implicit Euler differencing.

5. NUMERICAL EXPERIMENTS

We consider a domain $(x, y) \in [0, 2\pi]\times[0, 2\pi]$ with periodic boundary conditions. We use $f_0 = 2\pi$ and $c_0 = 4\pi^2$. The mean layer-depth is $H_0 = 1$. These parameter values correspond to a Rossby deformation radius of $L_R = 1$ and a Froude number of $\varepsilon = 1/(2\pi)$. The latitude θ is chosen such that one rotation of the plane (one "day") in physical time corresponds to one time unit in the computational model (i.e. $\sin\theta = 1/2$).

The initial conditions are defined as follows. We first introduce a PV field $\bar{q}$. See below for specific choices. This field is then used to provide an initial layer-depth perturbation via

$$\bar{\eta} = \varepsilon^{-1}\left(\frac{1}{1+\varepsilon\bar{q}} - 1\right) + k_0$$

where the constant k_0 is chosen such that η has a mean value of zero. The initial (purely geostrophic) velocity field is defined by

$$\mathbf{u} = L_R\boldsymbol{\nabla}_{\boldsymbol{x}}^\perp\bar{\eta}, \qquad \text{and} \qquad \mathbf{v} = \mathcal{S}_\alpha^p\mathbf{u}.$$

Next we define the (balanced) initial layer depth variation

$$\eta = -L_R^{-1}\nabla_{\boldsymbol{x}}^{-2}\nabla_{\boldsymbol{x}}\cdot(\omega\mathbf{v}^{\perp}).$$

These initial values finally imply a PV field $q = (L_R\zeta - \eta)/(1+\varepsilon\eta)$ and $\eta - \eta^{\mathrm{g}} = \delta^{\mathrm{s}} = 0$. The Lagrangian particles are initially placed on a uniform grid.

The following diagnostic variables are all evaluated over gridded Eulerian variables $\{\eta_{ij}\}$, $\{\mathbf{u}_{ij}\}$, $\{\mathbf{v}_{ij}\}$ etc. We define the discrete total energy

$$\mathcal{E}_\alpha(t_n) = \frac{L^2}{2N^2}\sum_{i,j}\mathbf{u}_{ij}(t_n)\cdot\mathbf{v}_{ij}(t_n) + 2\varepsilon^{-1}\left[(1+\varepsilon\eta_{ij}(t_n))(\ln(1+\varepsilon\eta_{ij}(t_n))-1)+1\right],$$

where $L = 2\pi$ is the domain length and N is the number of Fourier modes in the x and y direction. We monitor the relative error in the total energy

$$\delta E_\alpha(t_n) = \frac{\mathcal{E}_\alpha(t_n)-\mathcal{E}_\alpha(0)}{\mathcal{E}_\alpha(0)}.$$

We also compute the (approximate) L_2-norm of the smoothed divergence field $\{\delta^{\mathrm{s}}_{ij}\}$, i.e.

$$\langle\delta^{\mathrm{s}}\rangle_2 = \frac{L}{N}\left(\sum_{ij}(\delta^{\mathrm{s}}_{ij})^2\right)^{1/2},$$

as a measure of the ageostrophic component in the solution. Furthermore, one can define a balanced divergence field δ^{sg} to order $\mathcal{O}(\varepsilon)$ in the following manner [10]. Differentiate equation (18) with respect to time and multiply through by ε. This yields

$$\begin{aligned}\varepsilon^2\delta_{tt} &= -\varepsilon\nabla_{\boldsymbol{x}}^2\eta_t + \varepsilon L_R^{-1}\mathcal{S}_\alpha^p\zeta_t + \mathcal{O}(\varepsilon^2)\\ &= \nabla_{\boldsymbol{x}}^2\left(\delta^{\mathrm{s}} + \varepsilon\nabla_{\boldsymbol{x}}\cdot(\eta\mathbf{v}^{\mathrm{g}})\right) - L_R^{-2}\mathcal{S}_\alpha^p\left(\delta^{\mathrm{s}} + \varepsilon L_R\nabla_{\boldsymbol{x}}\cdot(\zeta\mathbf{v}^{\mathrm{g}})\right) + \mathcal{O}(\varepsilon^2).\end{aligned}$$

Next we ignore all terms of order $\mathcal{O}(\varepsilon^2)$ and take note of $\mathbf{v}^{\mathrm{g}}\cdot\nabla_{\boldsymbol{x}}\eta = 0$ as well as $\nabla_{\boldsymbol{x}}\cdot\mathbf{v}^{\mathrm{g}} = 0$ to obtain the defining relation

$$\left(1 - L_R^2\nabla_{\boldsymbol{x}}^2\mathcal{S}_\alpha^{-p}\right)\delta^{\mathrm{sg}} = -\varepsilon L_R\mathbf{v}^{\mathrm{g}}\cdot\nabla_{\boldsymbol{x}}\zeta = -\mathbf{v}^{\mathrm{g}}\cdot\nabla_{\boldsymbol{x}}\omega.$$

Thus we also monitor the (approximate) L_2 norm of the unbalanced divergence $\{\delta^{\mathrm{sag}}\}_{ij} = \{\delta^{\mathrm{s}} - \delta^{\mathrm{sg}}\}_{ij}$.

We used the time-stepping method (22) for the Eulerian wave part with a time-step of $\delta t = 1/N$, N the number of Fourier modes, and a radial basis function

$$\psi(r^2) = \left(\frac{1}{(r/r_0)^2 + c^2}\right)^4, \qquad r_0 = 2\Delta x,\ c = 1,$$

for the vorticity advection. A cut-off radius of $r_c = 2r_0$ was applied to limit the computational complexity in the summation (23).

The overall scheme was implemented using MATLAB and mex-subroutines for computing the interpolation operators and the radial basis functions over the Lagrangian particle locations.

5.1. Experiment A. Balanced two-vortex interaction

As a simple test case, we define a PV field as a sum of Gaussian pulses

$$\bar{q}(x,y) = \sum_{\ell=1}^{l} \alpha_\ell \exp\left(-\beta_\ell \left\{(x-x_\ell)^2 + (y-y_\ell)^2\right\}\right).$$

For this experiment we choose $l = 2$ and

$$\begin{array}{llll} \alpha_1 = 1, & \beta_1 = 12/L, & x_1 = 0.5, & y_1 = 0.5, \\ \alpha_2 = 1, & \beta_2 = 12/L, & x_2 = -0.5, & y_2 = -0.5, \end{array} \tag{27}$$

This field, representing two positively oriented vortices that are initially separated, is used to initialize the other variables as described in the previous section.

We first investigate the influence of the smoothing parameter α and the exponent p by performing a sequence of experiments over a time interval $t \in [0, 10]$ using the BPM method with $N = 64$ Fourier modes in each spatial direction and $M = 16N^2$ Lagrangian particles. The smoothing effect of the regularized formulation can be clearly seen from Fig. 1. But it is also apparent that choosing α too large can have an impact on the large scale rotation rate of the vortex pair.

The simulation is now repeated over a time interval $t \in [0, 15]$ using an Eulerian grid with $N = 128$ Fourier modes in each spatial direction. We use $M = 36N^2$ Lagrangian particles and a smoothing length $\alpha = 2\Delta x$. We set $p = 2$ in (13). The time evolution of the PV field can be found in Fig. 2 and diagnostic results in Fig. 3. The initial energy is $\mathcal{E}_\alpha = 0.6911$. Note the excellent conservation of the unbalanced divergence.

5.2. Experiment B. "Barotropic Instability"

As a second experiment, we consider a barotropic instability as a more challenging test for our method. In particular, we use

$$\bar{q}(x,y) = 4ye^{-2y^2}(1 + 0.1\sin(2x)).$$

The layer-depth variation, the velocity and PV field are then obtained as described above.

The simulation is run over a time interval $t \in [0, 15]$ using an Eulerian grid with $N = 128$ Fourier modes in each spatial direction. The initial energy is $\mathcal{E}_\alpha = 5.6117$.

5.2.1. The BPM method

We use $M = 36N^2$ Lagrangian particles and a smoothing length $\alpha = 4\Delta x$. We set $p = 2$ in (13). The time evolution of the PV field can be found in Fig. 4 and diagnostic results in Fig. 3. Note again the excellent conservation of the unbalanced divergence.

5.2.2. The PS method

We used the same number of Fourier modes and the same smoothing parameters. The PS method (25) was found to generate a large amount of noise in the PV field when integrated without hyperviscosity. Added hyperviscosity, as described in §4, improved the performance of the scheme. The time evolution of the PV field is shown in Fig. 5. It is quite apparent that the added hyperviscosity smears out some of the finer structures in the PV field.

The generalized enstrophies (10) are exactly conserved for the BPM method. This is not the case for the PS method and we monitor the relative error in the enstrophy $\mathcal{Q}_2$, which we discretize by

$$\mathcal{Q}_2(t_n) = \frac{L^2}{N^2}\sum_{i,j}\omega_{ij}(t_n)q_{ij}(t_n).$$

Conservation of enstrophy, energy and balance can be seen in Fig. 3. Note the excellent conservation of energy with a relative error of less than 10^{-4} at $t = 15$. The divergence field shows an almost identical behavior to the results from the BPM method.

6. CONCLUSIONS

Standard pseudospectral spatial discretization combined with a LF/TR time-discretization is unsuitable, in general, for long time simulations of geophysical flows, due to the artificial measures required to keep them stable [4, 3].

In this paper we have derived a set of regularized shallow-water equations and applied two different discretization methods. The application of the LF/TR method to the pseudospectral approximation of the regularized equations still requires the application of hyperviscosity which eliminates fine structures in the PV field. However, the method conserves energy and balance very well, requires a minimum number of FFTs, and is easy to implement. The newly proposed BALANCED PARTICLE-MESH method shows very promising results in term of PV advection and conservation of balance. A pseudospectral discretization of the semi-linear wave equation (20) requires about the same number of FFTs as the pseudospectral discretization of (15)–(16). However, we also have to update the particle locations and to evaluate the absolute vorticity using the radial basis function approximation. We expect that the application of multiple-time-stepping and averaging [11] will allow one to use larger time-steps for the particle advection.

One should also carefully investigate the effect of various types of radial basis functions and the effect of the cut-off radius on the approximation properties. This also includes the implementation of rapid evaluation strategies for (23).

We believe that a slightly reformulated version of the BPM method would be possible for nonrotating flows. This involves taking the formal limit $L_R \to \infty$ in this paper. In this case, the general approach described is suitable for adaptation to spherical geometry. The Eulerian grid functions should be expanded in spherical harmonics to avoid difficulties at the pole, and the Lagrangian advection can be handled by standard methods for constrained dynamics.

The results could also be extended to the primitive equations [14]

$$\begin{aligned}
\varepsilon\frac{d}{dt}\mathbf{u} &= -L_R^{-1}\mathbf{u}^{\perp} - \boldsymbol{\nabla}_{\boldsymbol{x}}B,\\
\varepsilon\frac{d}{dt}\eta &= -(1+\varepsilon\eta)\boldsymbol{\nabla}_{\boldsymbol{x}}\cdot\mathbf{u},\\
0 &= \eta + B_{\theta\theta}
\end{aligned}$$

where $\boldsymbol{x} = (x,y)^T$, θ is the potential temperature, $\mathbf{u} = (u,v)^T \in \mathbf{R}^2$ is the velocity field, and B is the pressure.

REFERENCES

[1] O. Bühler & M.E. McIntyre, On non-dissipative wave-mean interactions in the atmosphere or ocean, *J. Fluid Mech.* **354** (1998) 301–343.

[2] D. G. Dritschel & A. R. Mohebalhojeh, The contour-advection semi-Lagrangian algorithm: keeping the balance, Report, (2000).

[3] D.G. Dritschel, L.M. Polvani, & A.R. Mohebalhojeh, The contour-advective semi-Lagrangian algorithm for the shallow water equations, *Mon. Weather Rev.* **127** (1999) 1551–1565.

[4] D.R. DURRAN, *Numerical Methods for Wave Equations in Geophysical Fluid Dynamics*, (Springer-Verlag, New York, 1999).

[5] F.H. Harlow, The particle-in-cell computing methods for fluid dynamics, *Methods Comput. Phys.* **3** (1964) 319–343.

[6] R. W. Hockney & J. W. Eastwood, *Computer Simulation Using Particles*, (Adam Hilger, Bristol, New York, 1988).

[7] D. D. Holm, Fluctuation effects on 3D Lagrangian mean and Eulerian mean fluid motion, *Physica D* **133** (1999) 215–269.

[8] S. Kouranbaeva & M. Oliver, Global well-posedness for the averaged Euler equations in two dimensions., *Physica D* **138** (2000) 197–209.

[9] A.J. Majda & P. Embid, Averaging over fast gravity waves for geophysical flows with unbalanced initial data, *Theoret. Comput. Fluid Dynamics*, **11** (1997) 155-169.

[10] M. E. McIntyre & W. A. Norton, Potential vorticity inversion on a hemisphere, *J. Atmos. Sci.* **37** (2000) 1685–1699.

[11] B. Leimkuhler & S. Reich, A reversible averaging integrator for multiple time-scale dynamics, *J. Comput. Phys.* (in press).

[12] A. R. Mohebalhojeh & D. G. Dritschel, On the representation of gravity waves in numerical models of the shallow-water equations, *Q. J. R. Meteorol. Soc.* **126** (2000) 669–688.

[13] J. J. Monaghan, Smoothed particle hydrodynamics, *Ann. Rev. Astron. Astrophys.* **30** (1992) 543–574.

[14] R. Salmon, *Lectures on Geophysical Fluid Dynamics*, (Oxford University Press, Oxford, 1998).

[15] H. Yserentant, A new class of particle methods., *Numer. Math.* **76** (1997) 87–109.

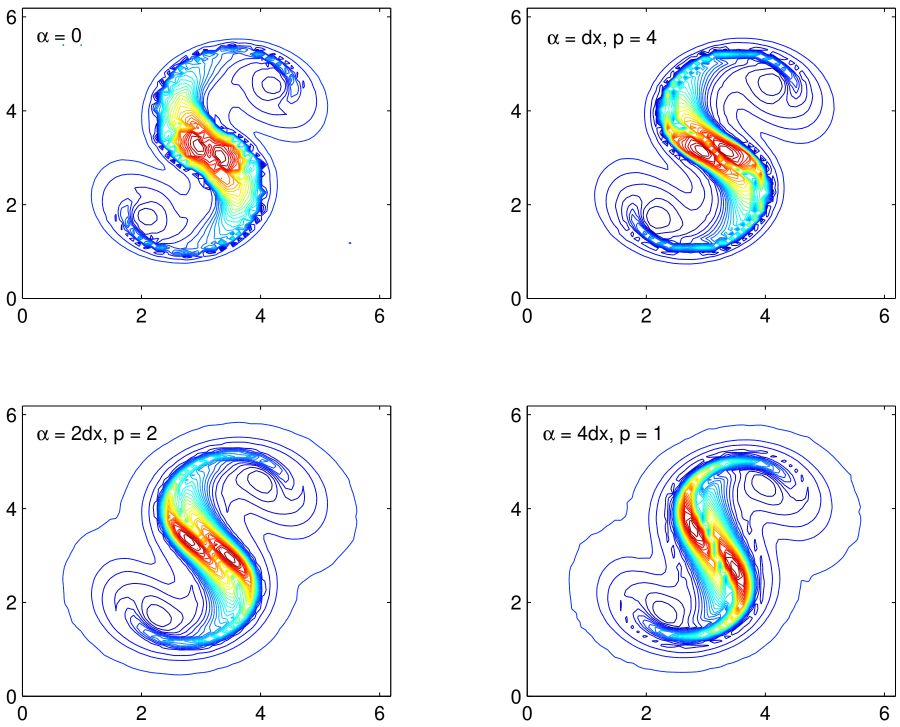

FIG. 1 Experiment A: PV field at $t = 10$ for various values of α and p in (13).

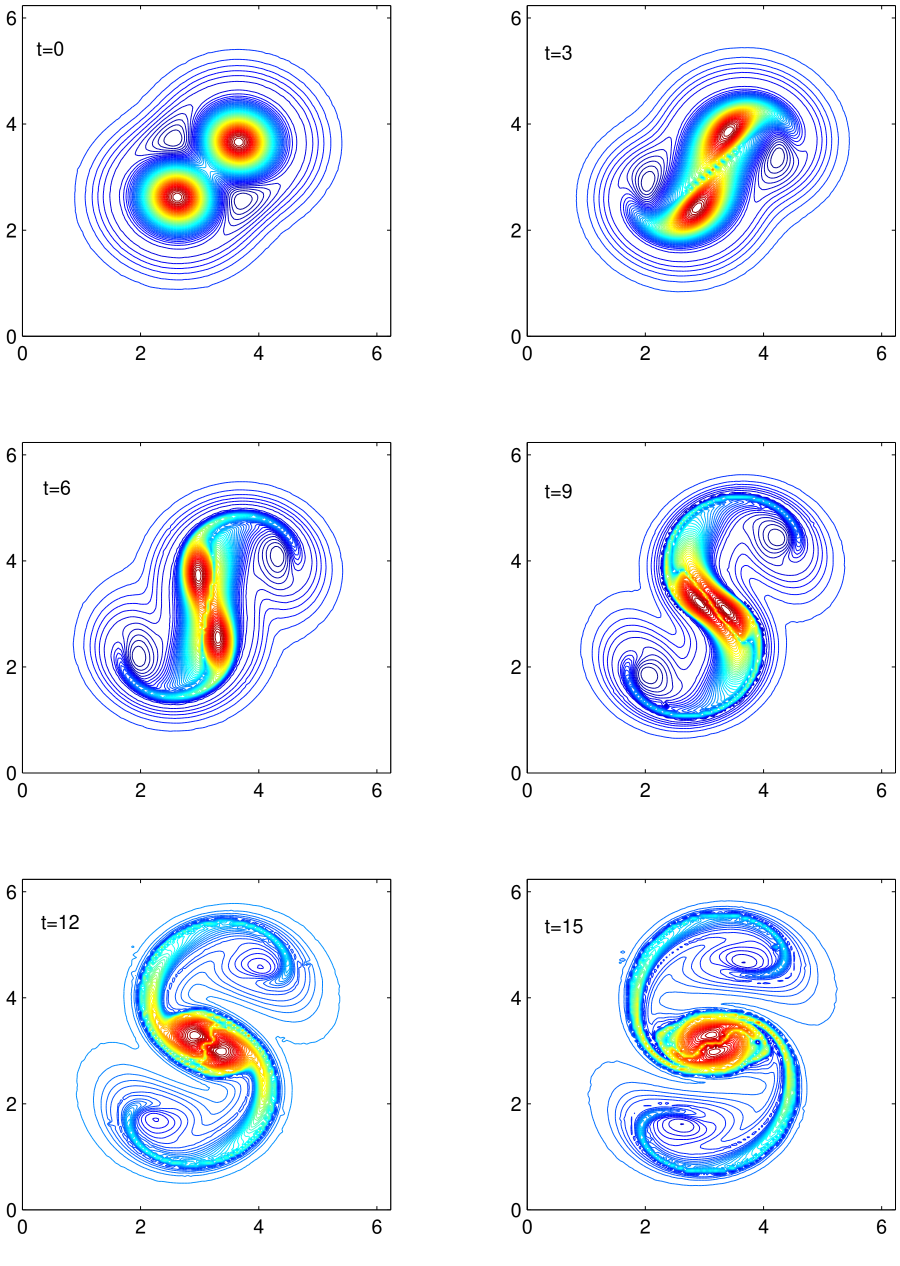

FIG. 2 Experiment A: PV field from BPM method.

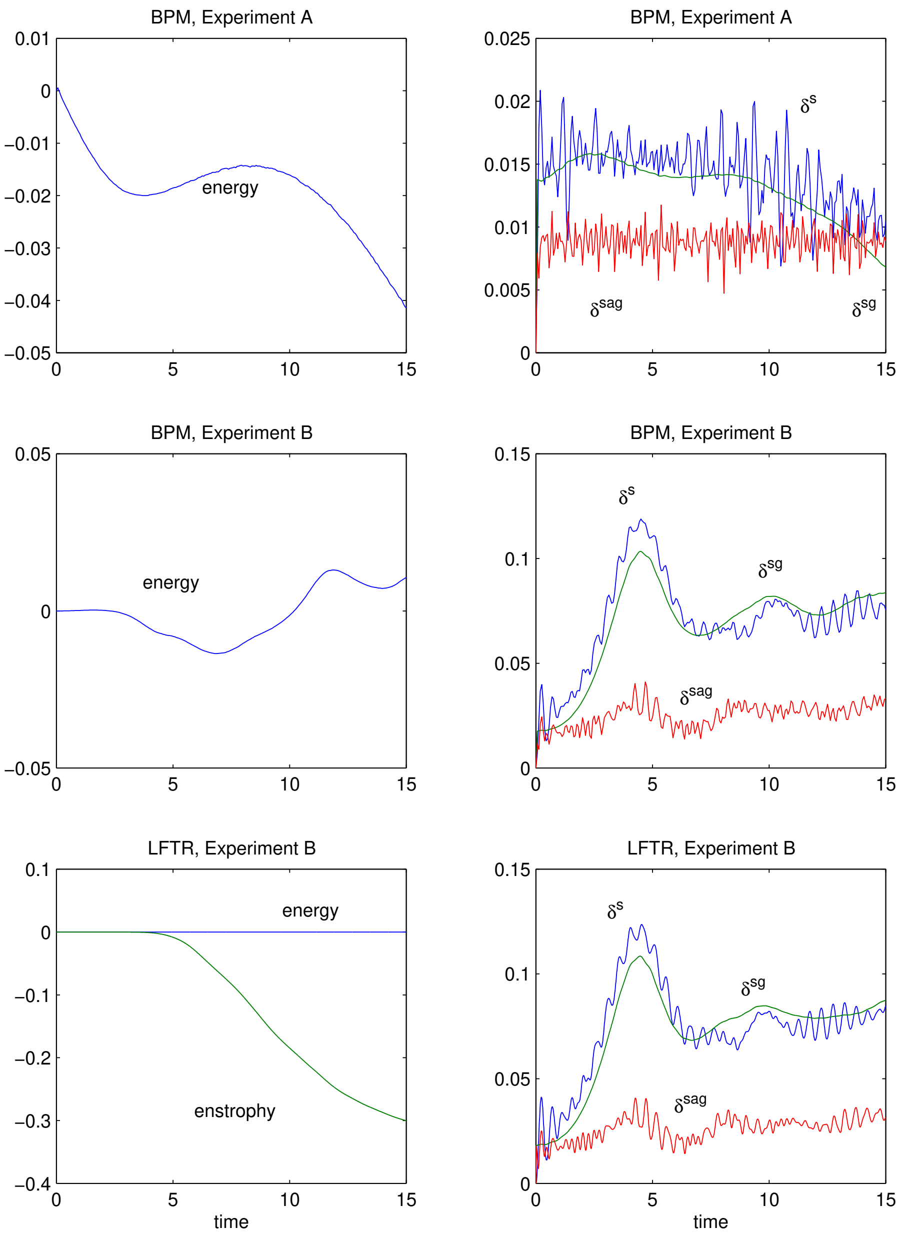

FIG. 3 Diagnostic for BPM and LF/TR method. The left column shows relative errors in energy (and enstrophy $\mathcal{Q}_2$ for the PS method) and the right column the L_2 norm of the divergence field

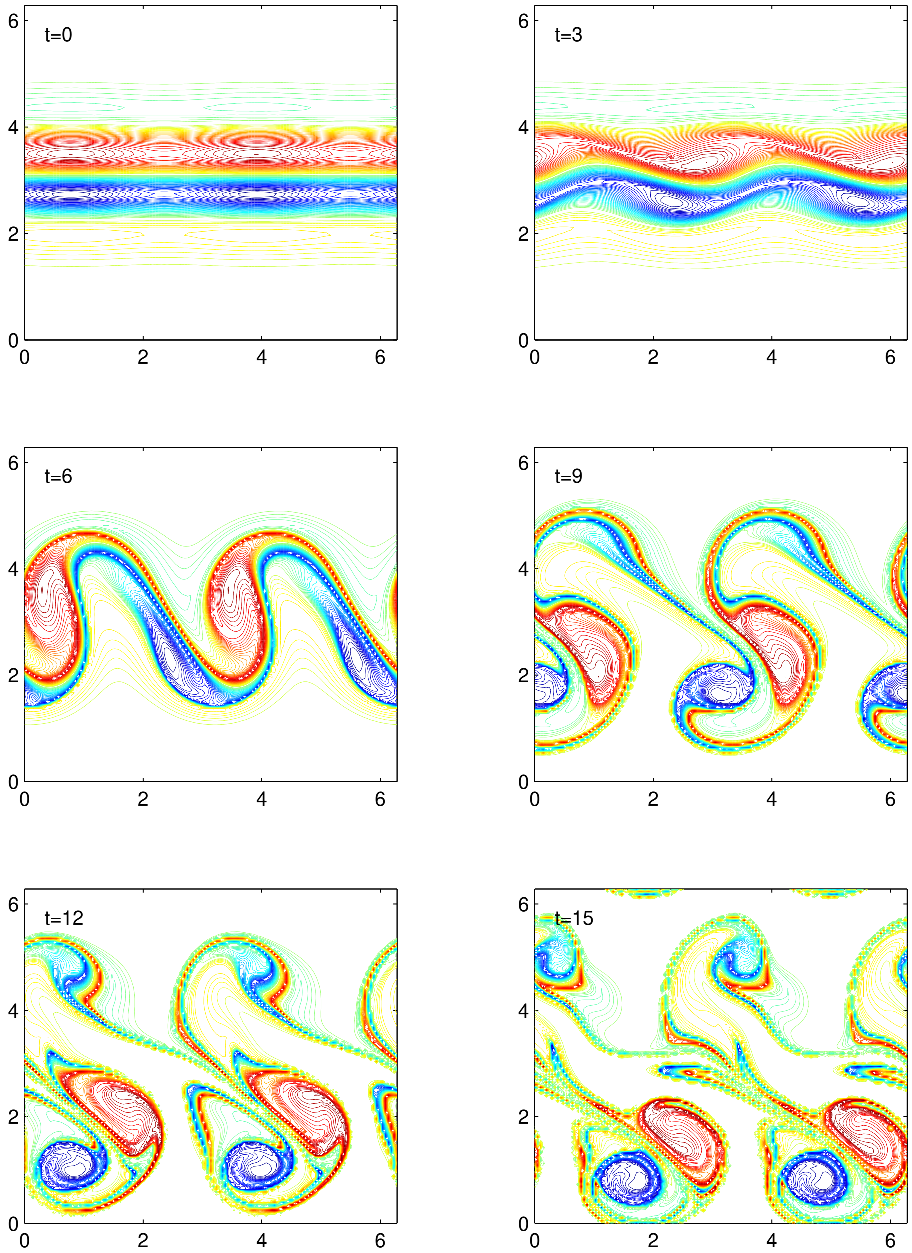

FIG. 4 Experiment B: PV field from BPM method.

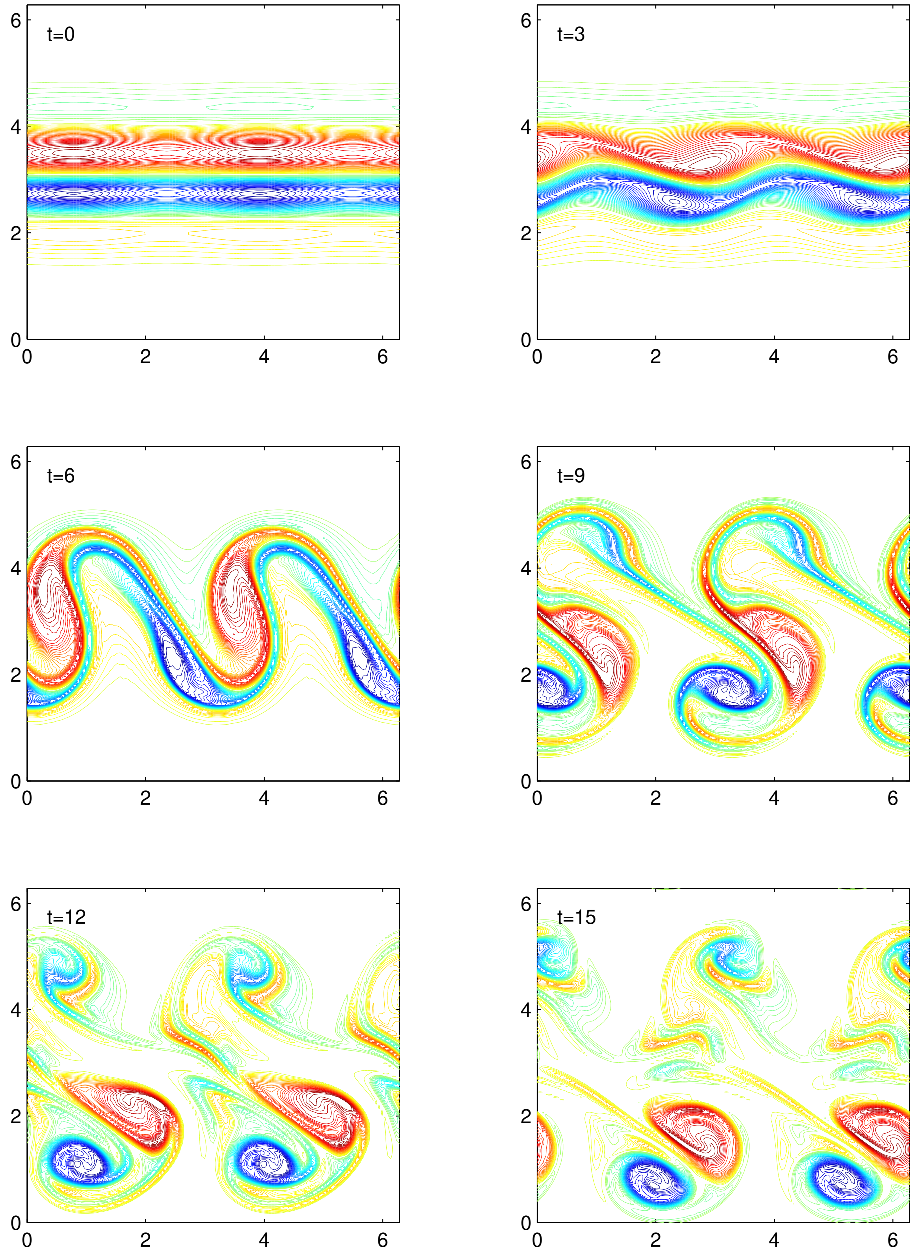

FIG. 5 Experiment B: PV field from LF/TR method with added hyperviscosity.